15th Triennial World Congress, Barcelona, Spain

DESIGN OF ROBUST CONTROLLERS FOR ACTIVE VEHICLE SUSPENSIONS

P. Gáspár [*] **I. Szászi** [**] **J. Bokor** [*]

[*] *Computer and Automation Research Institute, Kende u. 13-17, H-1111 Budapest, Hungary*
[**] *Budapest University of Technology and Economics, Műegyetem rkp. 3, H-1111 Budapest, Hungary*

Abstract: This paper is concerned with the design of robust controllers for active suspensions using μ methods, which take the structure of the model uncertainty into consideration. The complex μ method is conservative in the case of the real parametric uncertainty, while in the mixed μ method, both the real parametric and the complex uncertainties are handled together. Two half-car model structures are constructed, a rigid half-car model, and a high-order flexible one, which is more realistic and closer to the real situation. In the example, the result of the mixed μ method will be compared with the complex μ method and the traditional methods.

Keywords: Robust control, vehicle dynamics, uncertainty.

1. INTRODUCTION AND MOTIVATION

Active suspensions are used to provide good handling characteristics and to improve ride comfort while harmful vibrations caused by road irregularities and on-board excitation sources act upon the vehicle. The difficulties in the suspension design are that the performance requirements are usually in conflict, and that the model to be used in the control design contains uncertainties. The uncertainty of the model is caused by the neglected dynamics, high-order modes, uncertain components, inadequate knowledge of components. In the traditional methods, the uncertain components cannot be handled, thus robustness cannot be guaranteed in the presence of plant uncertainties. In the robust $\mathcal{H}_\infty$ synthesis the robust stability and performance can be guaranteed in the presence of unstructured uncertainty, however it often results in conservative controllers, Moran and Nagai (1992), Yamashita, et al. (1992), Park and Kim (1999). In the complex μ method, the structure of uncertainties is represented by a diagonal structure with full or scalar complex blocks. In practice, parametric uncertainties usually occur, thus they should be represented by repeated real blocks. In the mixed μ synthesis both the complex and the real uncertainties are taken into account, Balas and Doyle (1994), Gaspar, et al. (2001).

The aim of this paper is to apply the mixed μ synthesis to active suspension design, in which parametric uncertainties can be taken into account. Two half-car model structures are constructed in this paper, a rigid half-car model, and a high-order flexible one, which is more realistic and closer to the real situation. The control design is based on the rigid model, in which the handle of the complex and the real uncertainties are also included. The controller designed is tested using the flexible model. In the example, the result of the mixed μ method will be compared with the complex μ method and the traditional methods. The organization of the paper is as follows. Section 2 presents the concept of the active suspension design by using half-car models. Section 3 discusses the robust control design based on the mixed μ synthesis. Section 4 demonstrates the application of the μ synthesis in both the complex and mixed μ methods, and gives comparison results.

2. RIGID AND FLEXIBLE MODEL STRUCTURES FOR ACTIVE SUSPENSION

The well-known rigid half-car vehicle model, which is shown in Figure 1, is widely used for active suspension design. The model comprises three parts: the sprung mass and two unsprung masses. Let the sprung and unsprung masses be denoted by m_s, m_{uf}, m_{ur}, respectively. Both suspensions consist of a linear spring, a damper and an actuator to generate a pushing force between the body and axle. The front and rear suspension stiffness, the front and rear tire stiffness are denoted by k_{sf}, k_{sr} and k_{tf}, k_{tr}, respectively. The front and rear suspension dampings are denoted by b_{sf}, b_{sr}.

The half-car model is a four degrees-of-freedom system. The sprung mass is assumed to be a rigid body and has freedoms of motion in the vertical and pitch direction. The x_1 denotes the vertical displacement at the center of gravity and θ is the pitch angle of the sprung mass. The front and rear displacements of the sprung and the unsprung masses are denoted by x_{1f}, x_{1r} and x_{2f}, x_{2r}. In the model, the disturbances, w_f, w_r are caused by road irregularities. The input signals, f_f, f_r are generated by the actuators.

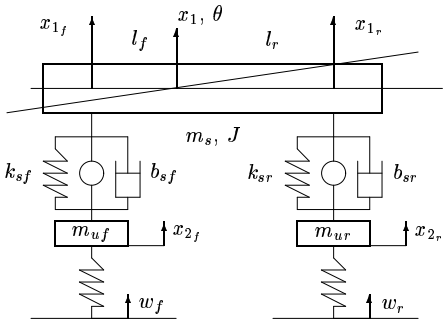

Fig. 1. Rigid half-car model

The parameters are assumed to be uncertain with a nominal value and a range of possible variation in the following way:

$$m_s = \bar{m}_s(1+d_{m_s}\delta_{m_s}), \quad k_i = \bar{k}_i(1+d_{k_i}\delta_{k_i}),$$

where $i \in \{sf, sr, tf, tr\}$ and d_{m_s}, d_{k_i} scalars, in which $-1 \le \delta_{m_s}, \delta_{k_i} \le 1$. The d scalar indicates the percentage of variation that is allowed for a given parameter around its nominal value. The changing of δ parameters in the interval $\begin{bmatrix}-1 & 1\end{bmatrix}$ determines the actual parameter deviation. All uncertainty parameters can be written in lower Linear Fractional Transformation (LFT) form. The m_s parameter occurs in the denominator of the motion differential equation, and the other uncertainty parameters such as k_i occur in the numerator. Their LFT representation can be represented in the following way:

$$\frac{1}{m_s} = \mathcal{F}_l\left(\begin{bmatrix} \frac{1}{\bar{m}_s} & -\frac{d_{m_s}}{\bar{m}_s} \\ 1 & -d_{m_s}\end{bmatrix}, \delta_{m_s}\right)$$
$$k_i = \mathcal{F}_l\left(\begin{bmatrix} \bar{k}_i & 1 \\ d_{k_i}\bar{k}_i & 0\end{bmatrix}, \delta_{k_i}\right);$$

The δ uncertainty blocks from the motion differential equations must be pulled out. Let the input and output of δ_{m_s} be y_{m_s} and u_{m_s}, and δ_{k_i} be y_{k_i} and u_{k_i}, respectively. Applying these formulae, the motion equation can be drawn up in the following way:

$$M\ddot{z} + B\dot{z} + Kz = Fu_\delta + K_r w + G_a f \tag{1}$$

where

$$z = \begin{bmatrix} x_1 & \theta & x_{2f} & x_{2r}\end{bmatrix}^T, w = \begin{bmatrix} w_f & w_r\end{bmatrix}^T, f = \begin{bmatrix} f_f & f_r\end{bmatrix}^T,$$
$$u_\delta = \begin{bmatrix} u_{m_s} & u_{k_{sf}} & u_{k_{sr}} & u_{k_{tf}} & u_{k_{tr}}\end{bmatrix}^T,$$

and the matrices are as follows:

$$M = \begin{bmatrix} M_s & 0 \\ 0 & M_u\end{bmatrix}, B = \begin{bmatrix} GB_sG^T & -GB_s \\ -B_sG^T & B_s\end{bmatrix}, G_a = \begin{bmatrix} -G \\ I\end{bmatrix},$$
$$K = \begin{bmatrix} GK_sG^T & -GK_s \\ -K_sG^T & K_s+K_t\end{bmatrix}, K_r = \begin{bmatrix} 0 \\ K_t\end{bmatrix}, F = \begin{bmatrix} F_1 \\ F_2\end{bmatrix}.$$

Here the sprung mass (M_s), the unsprung mass (M_u), the suspension stiffness (K_s), the tire stiffness (K_t), suspension damping (B_s), geometry (G) and (F_1, F_2) matrices are as follows:

$$M_s = \begin{bmatrix} \bar{m}_s & 0 \\ 0 & I_\theta\end{bmatrix}, M_u = \begin{bmatrix} m_{uf} & 0 \\ 0 & m_{ur}\end{bmatrix}, B_s = \begin{bmatrix} b_{sf} & 0 \\ 0 & b_{sr}\end{bmatrix},$$
$$K_s = \begin{bmatrix} \bar{k}_{sf} & 0 \\ 0 & \bar{k}_{sr}\end{bmatrix} K_t = \begin{bmatrix} \bar{k}_{tf} & 0 \\ 0 & \bar{k}_{tr}\end{bmatrix}, G = \begin{bmatrix} 1 & 1 \\ l_f & -l_r\end{bmatrix},$$
$$F_1 = \begin{bmatrix} \begin{bmatrix} -d_{m_s} \\ 0\end{bmatrix} & G & 0\end{bmatrix}, F_2 = \begin{bmatrix} 0 & I & I\end{bmatrix}$$

Using the differential equation (1) the state equation can be formulated in the following way:

$$\dot{x} = \hat{A}x + \hat{B}_1 w_\delta + \hat{B}_2 f \tag{2}$$

where

$$x = \begin{bmatrix} z^T & \dot{z}^T\end{bmatrix}^T, \quad w_\delta = \begin{bmatrix} u_\delta^T & w^T\end{bmatrix}^T$$
$$\hat{A} = \begin{bmatrix} 0 & I \\ -M^{-1}K & -M^{-1}B\end{bmatrix},$$
$$\hat{B}_1 = \begin{bmatrix} 0 & 0 \\ M^{-1}F & M^{-1}K_r\end{bmatrix}, \quad \hat{B}_2 = \begin{bmatrix} 0 \\ M^{-1}G_a\end{bmatrix}$$

The front and rear accelerations of the sprung masses are measured from their static equilibrium positions, (y_0). Moreover, (y_δ) is expressed as the inputs of δ blocks: $y_\delta = \begin{bmatrix} y_{m_s} & y_{k_s}^T & y_{k_t}^T\end{bmatrix}^T$, where

$$y_o = G^T\begin{bmatrix}\ddot{x}_1 & \ddot{\theta}\end{bmatrix}^T$$
$$y_{m_s} = \tilde{G}B_s(\dot{x}_u - \dot{x}_s) + \tilde{G}K_s(x_u - x_s) - \tilde{G}f + \tilde{F}_1 u_\delta,$$
$$y_{k_s} = D_{k_s}K_s(x_u - x_s),$$
$$y_{k_t} = D_{k_t}K_t(x_u - w)$$

Using the above expressions the output equation can be formulated in the following way:

$$y = \hat{C}_2 x + \hat{D}_{21} w_\delta + \hat{D}_{22} f \tag{3}$$

Similarly to the rigid half-car model, a high order flexible model is also constructed. This model is closer to the real system than the half-car model with an assumed rigid body. Then a ten-degree-of-freedom model is applied, see Fig. 2. In the model the lumped masses are located at each nodal point. It is assumed that the total body mass (M_s) is distributed in several nodal points. The mass distribution of the main body satisfies the decoupling condition, so the front and rear wheels are decoupled. The connection of the wheels

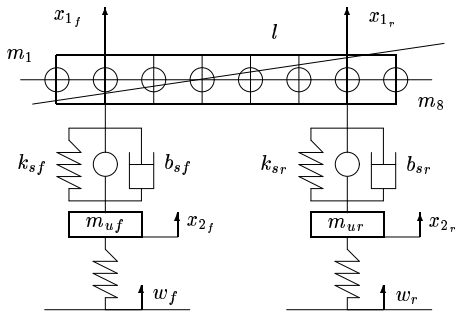

Fig. 2. Flexible half-car model

and the body are similar to the rigid body model, so the general structure of the differential equation will be similar to the equation (1). The most difficult part in the modeling of the flexible half-car model is the calculation of the stiffness of the elastic beam. The mathematical description of flexibility is computed using finite element methods. In the calculation the following assumptions are made: the structure of the sprung mass is established by the beam elements, the masses are lumped masses and located on the boundaries, the inertia of these masses is zero, the damping of the beam is assumed to be zero, and the relative axial displacement between the boundaries of the finite elements are small compared to the lateral displacement of the beam. The classical Bernouilli-Euler beam model is used for the flexible half-car model. The local variables of the beam element are the lateral displacement and rotations at the two ends. Thus, each joint has a lateral displacement (x) and a rotation (θ), which results in four coordinates for a beam element, Melosh (1990).

The stiffness matrix of the Bernouilli-Euler beam model can be determined by the area moment method:

$$\begin{bmatrix} F_A \\ T_A \\ F_B \\ T_B \end{bmatrix} = \frac{EI}{l^3} \begin{bmatrix} 12 & 6l & -12 & 6l \\ 6l & 4l^2 & -6l & 2l^2 \\ -12 & -6l & 12 & -6l \\ 6l & 2l^2 & -6l & 4l^2 \end{bmatrix} \begin{bmatrix} x_A \\ \theta_A \\ x_B \\ \theta_B \end{bmatrix} \tag{4}$$

where x_A and x_B indicate the displacements of the ends and θ_A and θ_B the rotations, respectively. Moreover, E represents the modulus of elasticity, I is the momentum of inertia, l is the length of a beam, F_i is the force at ends of the beam, and T_i is the momentum. The stiffness matrix is symmetric. Using (4) the rearranged stiffness matrix K_{ts} for the whole vehicle can be represented in the following generalized form:

$$\begin{bmatrix} F \\ T \end{bmatrix} = \frac{EI}{l^3} \begin{bmatrix} K_{11} & K_{12} \\ K_{21} & K_{22} \end{bmatrix} \begin{bmatrix} x \\ \theta \end{bmatrix}$$

Using those assumptions that the inertia of nodal masses are zero and the internal damping of the main body beam is zero, the rotational (θ) can be expressed by the vertical displacement (x) and the appropriate partitions of the stiffness matrix.

$$\theta = \frac{l^3}{EI} K_{22}^{-1} \left(T - \frac{EI}{l^3} K_{21} x \right) = -K_{22}^{-1} K_{21} x$$

Using this equation the force of beam elements can be represented in the following way:

$$F = \frac{EI}{l^3} \left(K_{11} - K_{12} K_{22}^{-1} K_{21} \right) x,$$

where the reduced stiffness matrix (K_b) is called the Schur complement of K_{11} in K_{ts}:

$$K_b = \frac{EI}{l^3} \left(K_{11} - K_{12} K_{22}^{-1} K_{21} \right).$$

The results will be applied to the flexible half-car model. The form of the state equation is similar to (1) with the following differences:

$$z = \begin{bmatrix} x_1 & \cdots & x_8 & x_{2f} & x_{2r} \end{bmatrix}^T$$

where the x_i ($i = 1, \ldots, 8$) is the vertical displacement of the beam elements. The sprung mass (M_s) and geometry (G) matrices and the total stiffness matrix (K) are as follows:

$$M_s = \begin{bmatrix} m_1 & & 0 \\ & \ddots & \\ 0 & & m_8 \end{bmatrix}; \quad G = \begin{bmatrix} 0 & 1 & 0 & 0 & 0 & 0 & 0 & 0 \\ 0 & 0 & 0 & 0 & 0 & 0 & 1 & 0 \end{bmatrix}^T$$

$$K = \begin{bmatrix} GK_sG^T + K_b & -GK_s \\ -K_sG^T & K_s + K_t \end{bmatrix}$$

3. ROBUST CONTROL BASED ON μ SYNTHESIS

Consider the closed-loop system in Figure 3, which includes the feedback structure of the model G and controller K, and elements associated with the uncertainty models and performance objectives. In the diagram, u is the control input, which is generated by actuators, y_o is the measured output, which contains the perturbed front and rear acceleration, w is the disturbance signal, which is caused by road irregularities, and n is the measurement noise. The $\tilde{z}$ represents the performance outputs, namely the vertical (z_a) and pitch (z_θ) acceleration, the suspension deflection (z_{sd}) and wheel travel (z_t) and the control input (z_u).

The parametric uncertainty of the sprung mass, suspension and tire stiffness are represented by the Δ_r block, whose input and output are u_δ, and y_δ. The transfer function Δ_r contains the $|\delta_{m_s}| < 1$, $|\delta_{k_i}| < 1$ ($i \in \{sf, sr, tf, tr\}$) components in diagonal form. The unmodelled dynamics is represented by W_r and Δ_m. It is assumed that the transfer function W_r is known, and it reflects the uncertainty in the model. The transfer function Δ_m is assumed to be stable and unknown with the norm condition, $\|\Delta_m\|_\infty < 1$. In the diagram, e is the input of the perturbation, d is its output. The weighting function W_n and W_w represent the impact of the different frequency domains in terms of sensor noise n and disturbance w, respectively. The weighting function W_p represents the performance outputs. The W_p contains the W_{p_i} ($i = 1, \ldots, 8$) components in diagonal form, which are related to the components of $\tilde{z}$.

Necessary and sufficient conditions for robust stability and robust performance can be formulated in terms of the structured singular value denoted as μ, Doyle (1985), Packard and Doyle (1993). Now, the design

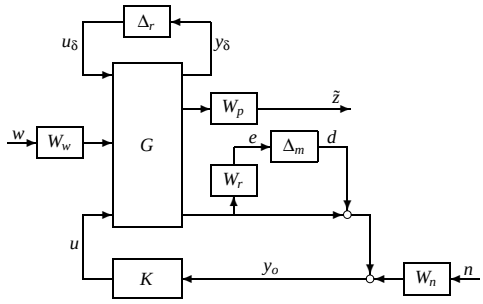

Fig. 3. Closed-loop interconnection structure

setup in Figure 3 is formalized as a standard design problem, i.e. the so-called $P-K$ structure where,

$$\tilde{d} = \begin{bmatrix} u_\delta & d \end{bmatrix}^T, \quad \tilde{w} = \begin{bmatrix} w & n \end{bmatrix}^T, \quad \tilde{e} = \begin{bmatrix} y_\delta & e \end{bmatrix}^T,$$
$$\tilde{z} = \begin{bmatrix} z_a & z_\theta & z_{sd} & z_{td} & z_u \end{bmatrix}^T$$

The mixed real and complex μ involves three types of blocks: repeated real scalar, repeated complex scalar and full blocks. The admissible set of uncertainties $\tilde{\Delta}$ is defined as

$$\tilde{\Delta} = \begin{bmatrix} \Delta_r & 0 & 0 \\ 0 & \Delta_m & 0 \\ 0 & 0 & \Delta_p \end{bmatrix},$$

where $\Delta_r \in \mathbb{R}^{5\times 5}$, $\Delta_m \in \mathbb{C}^{2\times 2}$, $\Delta_p \in \mathbb{C}^{4\times 8}$. The first block, Δ_r is a repeated real scalar block which represents the parametric uncertainties. The second block of this structured set corresponds to the scalar-block uncertainty Δ_m, which is used to describe the unmodelled dynamics. The Δ_p is a fictitious uncertainty block, which is used to incorporate the $\mathcal{H}_\infty$ nominal performance objective into the μ framework. Given a matrix $M = \mathcal{F}_l(P,K)$, the mixed $\mu_{\tilde{\Delta}}$ function is then defined by:

$$\mu_{\tilde{\Delta}}(M) := \frac{1}{\min\{\bar{\sigma}(\Delta) : \Delta \in \tilde{\Delta}, \det(I - M\Delta) = 0\}}$$

unless no $\Delta \in \tilde{\Delta}$ makes $I - M\Delta$ singular, in which case $\mu_\Delta(M) = 0$. Thus $1/\mu_{\tilde{\Delta}}(M)$ is the "size" of the smallest perturbation Δ, measured by its maximum singular value, which makes $\det(I - M\Delta) = 0$. Unfortunately this equation is not suitable for computing μ since the implied optimization problem may have multiple local maxima. However tight upper and lower bounds for μ may be effectively computed for both complex and mixed perturbation sets. Algorithms for computing these bounds have been documented in several papers, see e.g. Balas et al. (1991). Define

$$\mathcal{Q} = \left\{\Delta \in \tilde{\Delta} : \phi_i \in [-1,1], |\delta_i| = 1, \Delta_i \Delta_i^* = I_{m_i}\right\}$$
$$\mathcal{D} = \left\{ \begin{array}{c} \mathrm{diag}\left[\tilde{D}_1, \tilde{D}_2, \tilde{D}_3, \tilde{D}_4, \tilde{D}_5, d_1 I_1, I_2\right] : \\ \tilde{D}_1 \in \mathbb{C}^{1\times 1}, \tilde{D}_2 \in \mathbb{C}^{1\times 1}, \tilde{D}_3 \in \mathbb{C}^{1\times 1}, \\ \tilde{D}_4 \in \mathbb{C}^{1\times 1}, \tilde{D}_5 \in \mathbb{C}^{1\times 1} \\ d_1 \in \mathbb{R}, I_1 = I^{2\times 2}, I_2 = I^{4\times 8} \end{array} \right\}$$
$$\mathcal{G} = \left\{ \begin{array}{c} \mathrm{diag}\left[G_1, G_2, G_3, G_4, G_5, 0, 0\right] : \\ G_1 \in \mathbb{C}^{1\times 1}, G_2 \in \mathbb{C}^{1\times 1}, G_3 \in \mathbb{C}^{1\times 1}, \\ G_4 \in \mathbb{C}^{1\times 1}, G_5 \in \mathbb{C}^{1\times 1} \end{array} \right\}$$

The lower bound for mixed μ is as follows:

$$\max_{Q\in\mathcal{Q}} \rho_R(QM) \le \mu_{\tilde{\Delta}}(M).$$

where $\rho_R(QM)$ is the real spectral radius of QM.

The lower bound is actually an equality but unfortunately the function $\rho_R(QM)$ is non-convex so we cannot guarantee to find the global maximum and hence we only obtain the lower bound for μ. The upper bound can be formulated as a convex optimization problem, so the global minimum can be found. For a constant matrix M and both complex and mixed uncertainty structure $\tilde{\Delta}$, an upper bound for $\mu_{\tilde{\Delta}}(M)$ that take the phase information of the real parameters into account can be formulated into an optimization problem:

$$\inf_{D\in\mathcal{D}, G\in\mathcal{G}} \min_{\beta} \left\{\beta \mid M^*DM + j(GM - M^*G) - \beta^2 D \le 0\right\}$$

Using this upper bound, the optimization is reformulated as

$$\min_K \sup_\omega \inf_{D\in\mathcal{D}, G\in\mathcal{G}} \min_\beta \{\beta \mid \quad \bar{\sigma}(\Gamma(\omega)) \le 1)\}$$

where

$$\Gamma(\omega) = \left(\frac{D_\omega F_l(P,K)(j\omega) D_\omega^{-1}}{\beta} - jG_\omega\right)(I + G_\omega^2)^{-\frac{1}{2}}$$

and D_ω, G_ω are selected from the set of scaling $\mathcal{D}$, $\mathcal{G}$ independently of every ω.

The scaling G allows the exploitation of the phase information about the real parameters so that a better upper bound can be obtained. The optimization problem can be solved in an iterative way using for D, G and K. For fixed $K(s)$ the problem of finding $D(\omega)$, $G(\omega)$ and β is just the mixed upper bound problem. Having found these scalings $\beta^* = \max\beta$ might be fixed and transfer function matrices $D(s)$ and $G(s)$ to $D(\omega)$ and $jG(\omega)$ might be fitted. It can be shown that using spectral factorization, a stable interconnection $P_{DG}(s)$ can be formed, which approximates $\Gamma(\omega)$ across frequency ω. For given β^*, $D(s)$ and $G(s)$ the problem of finding the controller $K(s)$ will be reduced to a standard $\mathcal{H}_\infty$ problem. The procedure is called $D,G-K$ iteration.

4. DEMONSTRATION EXAMPLE

In the demonstration example, the suspension design is based on the rigid half-car model, and the compensator designed is tested in the flexible half-car model. Thus, the rigid model is the basis of the design and the flexible model represents the actual plant. The nominal parameters are the following:
$m_s = 580kg, I_\theta = 1100kgm^2, m_{uf} = 40kg, m_{ur} = 40kg,$
$k_{sf} = 23500N/m, k_{sr} = 25500N/m, k_{tf} = 190000N/m,$
$k_{tr} = 190000N/m, b_{sf} = 1000N/m/s, b_{sr} = 1100N/m/s.$ In the example, the dynamics of the hydraulic actuator is modelled as $G_a(s) = \frac{1}{1/75s+1}$. The open loop frequency responses of the rigid model and the flexible model are illustrated in Figure 4. The parameters are assumed to be uncertain, with a nominal value and a range of possible variation: $d_{ms} = 0.2, d_{ksf} = 0.15, d_{ksr} = 0.15, d_{ktf} = 0.25, d_{ktr} = 0.25$. Note that this represents 20% uncertainty in m_s, 15% uncertainty in k_{sf} and k_{sr}, moreover 25% uncertainty in k_{tf} and k_{tr}.

In preparation for the control design, the uncertainty weighting function W_R and the performance weighting

function W_P must be selected. In the complex μ synthesis uncertainty is modelled as a complex full block with multiplicative uncertainty at the plant input. Let the frequency weighting function of the unmodelled dynamics be as follows: $W_R^1 = 1.875\frac{S+2}{S+25}$, which is illustrated by the dotted line in the right hand side of Figure 5. In the mixed μ synthesis, in which mixed uncertainty is applied, information about the model uncertainties between the model and the plant must be used in the control design, and the magnitude of the unmodelled dynamics must be decreased. Thus, the weighting function W_R^2 can be selected significantly smaller than in the previous case: $W_R^2 = 0.2\frac{S+50}{S+200}$, which is illustrated by the solid line in Figure 5.

The purpose of weighting functions W_{p_1}, W_{p_2} and W_{p_3} is to keep the vertical and pitch acceleration moreover to keep the suspension deflection small over the desired frequency range. We choose $W_{p_1} = W_{p_2} = 0.2\frac{S+200}{S+50}$, and $W_{p_3} = \text{diag}\left[0.029\frac{S+350}{S+10}, 0.029\frac{S+350}{S+10}\right]$ for front and rear suspension, respectively. These weighting functions are illustrated in the left hand side of Figure 5. Let the frequency weighting function for the wheel travel be $W_{p_4} = \text{diag}\,[1,1]$. The magnitude of the control force is limited by the weighting function $W_{p_5} = \text{diag}\left[4\cdot 10^{-3}, 4\cdot 10^{-3}\right]$. The weight W_w is used to scale the magnitude of the road disturbance, which is chosen $W_w = 0.03$. The fact that the magnitude of the road excitation is 0.03 m entails that the effect of the disturbance signal on the control input will not exceed 48 dB. We set $W_n = 0.001$, thus essentially it is assumed that the sensor noise is 0.001 m/s^2 at the front and rear body acceleration in the whole frequency domain.

In the case of complex μ synthesis, the control design is performed by using the $D-K$ iteration. The important values of the steps of the iteration are shown in Table 1. As a result of Step 4, the compensator order is selected 52, and all the nominal performance, robust stability, and robust performance are achieved. In the case of mixed μ synthesis, the control design is performed by using the $D,G-K$ iteration method.

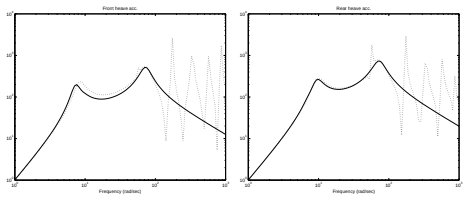

Fig. 4. Open-loop frequency response

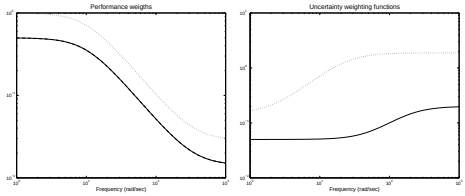

Fig. 5. Weighting functions

The values of the steps of the iteration are shown in Table 2. Because of Step 3, the compensator order is selected 68. The price of the mixed μ synthesis is usually a controller with larger order, which can be usually reduced. The controller reduction is based on the balanced realization and optimal Hankel norm approximation. This approach works well, since the poles have negative real part. The order of the controller is selected 20, in which all the nominal performance, the robust stability, and the robust performance are achieved.

Table 1. Summary of the D-K iteration

Iteration	#1	#2	#3	#4
Controller order	16	20	44	52
D-scale order	0	4	28	36
Gamma achieved	26.563	5.649	2.115	0.976
Peak μ value	7.821	2.346	1.000	0.962

Table 2. Summary of the D,G-K iteration

Iteration	#1	#2	#3
Controller order	16	32	68
D-scale order	0	16	30
G-scale order	0	0	22
Gamma achieved	5460.07	19.166	1.327
Peak μ value	44.253	1.413	0.991

The frequency responses of the controlled system, i.e. the vertical accelerations, the pitch accelerations, and the suspension deflection are illustrated in Figure 6. The solid line corresponds to the mixed μ synthesis, the dashed line to the complex μ synthesis, the dotted line to the LQG design, and the dashed-dotted line to the passive system. The first amplitude peak, which corresponds to the eigen-frequency of the body mass, is the largest in the passive system, and it practically disappears in the mixed μ design. The reduction in vertical and pitch acceleration in the low frequency range corresponds to the increase in the suspension deflection in this range. Since the tire-hop frequency is an invariant point (about $\omega_1 = 68.9$ rad/sec in this example), the acceleration responses are close to the passive response at this frequency and it cannot be decreased by feedback.

The designed compensators are verified in a real situation, which is represented by its application for the flexible structure. The time responses are illustrated in Figure 7. In the example, the input signal is simulated as a bump with 0.03 m maximal value. The effects of the disturbance on the sprung mass acceleration are seen as large oscillations with long duration in the case of complex μ control. The mixed μ control shows better properties in terms of both the value and the duration of the oscillation. The effects of the disturbance on the suspension deflection are great in the complex μ control. In the mixed μ case, the suspension deflection achieves its steady state value within a short time. The overshoot of the LQG control is the largest, however the duration is shorter than in the complex μ case. The input forces are similar in all cases.

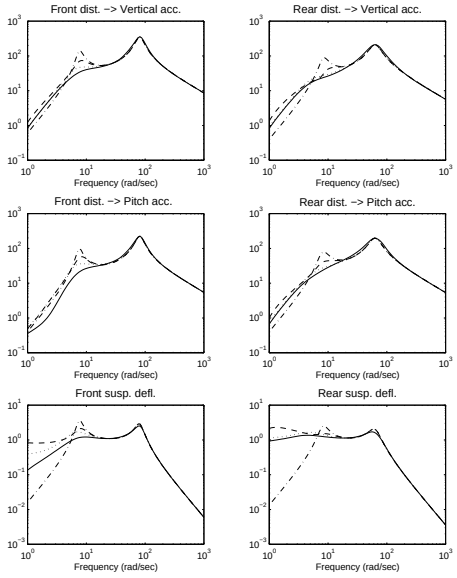

Fig. 6. Frequency responses of the designed system

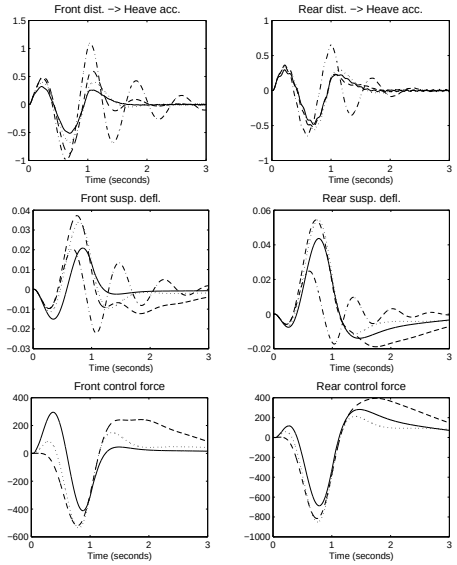

Fig. 7. Time responses of the actual system

5. CONCLUSIONS

In this paper, robust μ methods have been applied in the active suspension design. The result of the complex μ method is more conservative than that of the mixed μ method since, in the latter case, the real parametric uncertainties can be taken into consideration. The price of the mixed μ synthesis is usually a controller with larger order, which can be effectively reduced.

6. REFERENCES

[1] Balas, G. and J.C. Doyle ”Robustness and performance trade-offs in control design for flexible structures”, *IEEE Trans. Control Systems Technology*, Vol. 2, No. 4, 352-361., (1994)

[2] Balas, G., J.C. Doyle, K. Glover, A. Packard, and R. Smith ”μ analysis and synthesis toolbox”, *MUSYN Inc. and The Mathworks Inc.*, (1991).

[3] Doyle, J. ”Structured uncertainties in control system design”, *Proc. of the 24th Conference on Decision and Control*, Lauderdale, 260-265., (1985).

[4] Gaspar P., I. Szaszi, G.J. Balas, and J. Bokor ”Active suspension design based on mixed uncertainty modeling”, *European Control Conference, Porto*, 3624-3629., (2001).

[5] Hrovat, D. ”Optimal active suspension structures for quarter-car vehicle models”, *Automatica*, Vol. 26, 845-860., (1990)

[6] Melosh, R. J. ”Structural Engineering Analysis by Finite Elements”, *Prentice Hall*, New Jersey. (1990)

[7] Moran, A. and M. Nagai ”Performance Analysis of Vehicle Active Suspension with $\mathcal{H}_\infty$ Robust Control”, *Proc. of the 1st Int. Conf. on Motion and Vibration Control*, Yokohama, 756-761., (1992)

[8] Packard, A. and J. Doyle ”The complex structured singular value”, *Automatica*, Vol. 29, No. 1, 71-109., (1993)

[9] Park, J.H. and Y.S. Kim, ”An $\mathcal{H}_\infty$ controller for active suspensions and its robustness based on a full-car model”, *Proc. of the 14th World Congress of IFAC*, P-8b-02-3, (1999)

[10] Sharp, R.S. and D.A. Crolla ”Road Vehicle Suspension System Design - a review”, *Vehicle System Dynamics*, 16, 167-192., (1987)

[11] Thompson, A.G. and B.R. Davis ”Optimal linear active suspensions with derivative constraints and output feedback control”, *Vehicle System Dynamics*, 17, 179-192., (1988)

[12] Yamashita, M., K. Fujimori, K. Hayakawa, and H. Kimura ”Application of $\mathcal{H}_\infty$ control to active suspension system”, *Automatica*, 30, 1717-1729., (1994)